

# Four-channel multiplexer on surface plasmon polaritons development and research

**Nevinskyi D.V., Zakalyk L.I., Lebid S.Y., Korzh H.I., Pavlysh V.A.**

Lviv Polytechnic National University,  
Institute of Telecommunications, Radioelectronics  
and Electronic Engineering,  
2 Profesorska str., Lviv, 79013 Ukraine,  
e-mail: nevinskyi90@gmail.com

Simulation of the surface plasmon polariton (SPP) distribution in the 10 μm long four-channel multiplexer is conducted in present paper. The excitation of the SPP was done using the 632.8 nm pulse laser with 50 fs pulse duration. The simulation processes of the SPP propagation in the four-channel multiplexer were performed for the latter switched as a splitter as an adder. Though the obtained signal strength is low due to ohmic losses and signal reflections in the middle of the waveguide it is possible to register it. The detailed procedure of waveguides preparation, analysis and registration of SPP propagation is described in the paper. For the proposed model verification the two-channel 20 μm long splitter was formed by optical projection lithography. Studies have shown that the SPP is distributed throughout the whole structure of the 20 μm long two-channel splitter with a partial extinction due to ohmic losses.

**Keywords:** surface plasmon polariton, splitter, adder, model, lithography, channel, multiplexer

## Introduction

It can be seen that throughout the past several years a very active research aimed at the study of surface plasmon polaritons (SPP) is conducted, which opens up the prospect of a new generation of optical devices [1].

Various approaches to achieve effective excitation of SPP are proposed to date [2-5]. Geometrically limited channels for SPP distribution are also considered [6,7]. Manufacturing of nanoscale waveguides that provide a simple and cost-effective way to achieve strong side retention of SPP and implementation of integrated components are still in a state of ongoing research.

An SPP represent coherent oscillations of surface electrons of the metal at the interface metal-insulator and caused great interest in various fields of research in recent years [8]. An SPP with frequencies below the surface plasmon resonance of the metal-insulator transition are limited and can propagate along the waveguide. The SPP excitation on the metal surface opens up new possibilities for the use of their properties: for sensing and detection of single molecules in chemistry, biology and medicine, electronics, and information and communication technologies [9].

Side constraints in the plane of the metal surface, perpendicular to the direction of the SPP propagation are necessary to implement the compact plasmon devices and circuits.

Based on the full-wave finite-difference time-domain (FDTD) method, we carry out the numerical simulation on the transportation of SPP by using a commercial software package (Lumerical, FDTD\_Solutions).

The simulated propagation of the SPP in the four-channel multiplexer using 632.8 nm laser as a source of the optical signal is demonstrated in current paper and it was experimentally demonstrated that SPP can propagate in the dual-channel splitter geometrically bigger.

## Modeling of the SPP propagation

A physical model of the system based on dot-dipole approach was applied to explain the processes that occur during the formation of SPPs on the surface of nanosized metal film [10]. This method has some limitations, but this restriction allows to bypass the problems associated with energy scattering at the interface dielectric-film basis and take into account only the energy transfer between the particles.

The surface of the nanostructured metal film of gold was presented as a chain of strongly interacting atoms. The light is directed to the first atom in chain, the remaining are irradiated by the scattering energy from the first one. The polarization of the external field can be either S, or P. Thus, Maxwell's equations can be used to describe such a physical system and calculation could be carried out using Green function. The electric field in such a structure can be determined from the Lipmann-Schwinger equation:

$$E(r) = E^0(r) + k_0^2 \sum_{i=1}^N \int_{V_i} \hat{G}(r, r') (\epsilon_p - 1) E(r') dr' \quad (1)$$

where  $E^0$  – external electrical field in the starting point,

$k_0$  – ballistical wave vector,

$N$  – whole number of the particles in the chain;

$V_i$  – volume, which particle takes with  $i$  number;

$\hat{G}(r, r')$  - Green's tensor;

$\epsilon_p$  – dielectric constant Au.

The light propagation without particles is described by the Green's tensor  $\hat{G}(r, r')$ . In the dipole approximation, each nanoparticle is seen as a dipole reflector with dipole moment, which can be obtained by solving the following equations:

$$p_1 = \hat{a}_1 E^0(r_1) + \frac{k_0^2}{\varepsilon_0} \hat{a}_1 \hat{G}^S(r_1, r_1) p_1 + \\ + \frac{k_0^2}{\varepsilon_0} \sum_{j=1}^N \hat{a}_1 [\hat{G}^0(r_1, r_j) + \hat{G}^S(r_1, r_j)] p_j, \quad (2)$$

$$p_i = \frac{k_0^2}{\varepsilon_0} \hat{a}_i \hat{G}^S(r_i, r_j) p_i + \\ + \frac{k_0^2}{\varepsilon_0} \sum_{j \neq i}^N \hat{a}_i [\hat{G}^0(r_i, r_j) + \hat{G}^S(r_i, r_j)] p_j, i = 2, \dots, N, \quad (3)$$

where  $r_i = (x_i; y_i; z_i)$  – radius-vector of the  $i$ -th particle;  
 $\varepsilon_0$  – dielectric constant;  
 $\hat{a}_i$  – dimensionless tensor of the  $i$ -th particle.

Given the identity of the spherical particles with half-axis  $h_x, h_y, h_z$  and that they are parallel to the coordinate axes (see Fig. 1), the polarization tensor in the long-wave approximation is [11]:

$$a = (a_x \hat{x} \hat{x} + a_y \hat{y} \hat{y} + a_z \hat{z} \hat{z}), \quad (4)$$

where  $\hat{x}, \hat{y}, \hat{z}$  - coordinate unit vectors,

$$a_\tau = \frac{\varepsilon_0 V (\varepsilon_p - 1)}{1 + (\varepsilon_p - 1) m_\tau}, \tau = x, y, z \quad (5)$$

where  $V = 4\pi h_x h_y h_z / 3$  – particle volume,  
 $m_x, m_y, m_z$  – depolarization ratio.

Nanoparticles are at the basis of the dielectric, the Green tensor will  $\hat{G}^0(r, r')$  and  $\hat{G}^S(r, r')$ . The component  $\hat{G}^0(r, r')$  defines a value of the constant electric field, and  $\hat{G}^S(r, r')$  represents the field that is scattered on the metal-insulator transition.

Accordingly, the electric field on the metal surface can be described by the equation:

$$E(r) = k_0^2 \sum_{i=1}^N [\hat{G}^0(r, r_i) + \hat{G}^S(r, r_i)] p_i \quad (6)$$

$\hat{G}^0(r, r')$  tensor can be solved analytically [11]. In general, taking into consideration that particles in the chain are close to the interface and have size smaller than the wavelength, it makes mathematical method much simpler. In particular, if the distance between the source and the observation point is less than  $20\lambda$  — the Green tensor has the exact meaning, including all methods of dispersion and only part of the surface plasmon is approximated. Numerical calculations using this method is 5-7% accurate.

The alternative method to describe processes in waveguides through which SPP propagates, is the Monte Carlo method using the Green function [13].

### SPP propagation modeling in the four-channel multiplexer

The  $10 \mu\text{m} \times 5 \mu\text{m}$  structure with  $200 \text{ nm}$  channel thickness and  $180 \text{ nm}$  height is proposed to simulate the process

of SPP propagation in a multiplexer. The distance between the channels is  $1.5 \mu\text{m}$  (see Fig. 2).

As a result of the simulation process of the SPP propagation in the four-channel multiplexer switched as a splitter, the dependence of the SPP intensity on the distance is obtained. Entry of the splitter is excited with the  $632.8 \text{ nm}$  pulse laser and  $50 \text{ fs}$  pulse duration. SPP propagates in all four-channels of the multiplexer, although intensity slightly decreases at the distance of  $6 \mu\text{m}$  (Fig. 3).

The simulation result shows that the output intensity is attenuated due to the ohmic losses and split of the SPP, but received signal strength will be sufficient to identify it.

A modeling process of the SPP propagation in a multiplexer when it is switched as adder was also conducted. Each channel (there are four-channels) was excited by  $632.8 \text{ nm}$  pulse laser with  $50 \text{ fs}$  pulse duration and at a certain time. Each channel is allocated  $50 \text{ fs}$  of exposure time

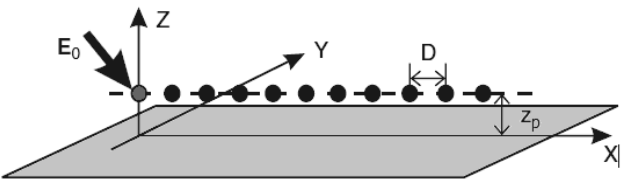


Fig. 1. Schematic drawing: long linear chain of identical spheroidal particles of gold [12]

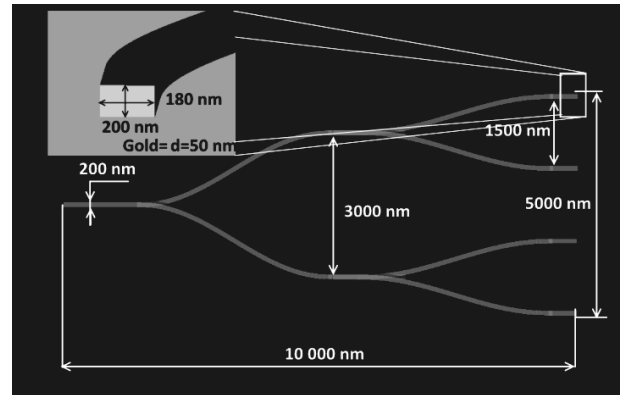


Fig. 2. Structural scheme of the multiplexer

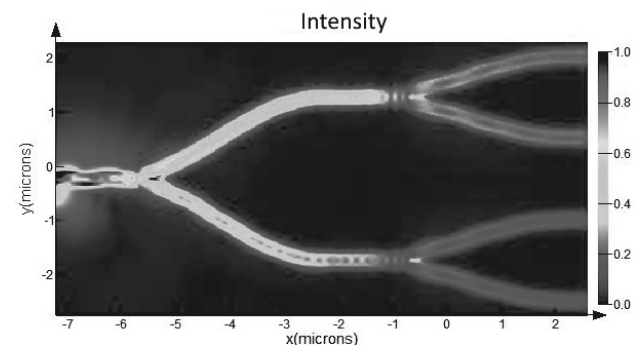


Fig. 3. The distribution of the intensity of SPP propagation along the four-channel multiplexer applied as a splitter

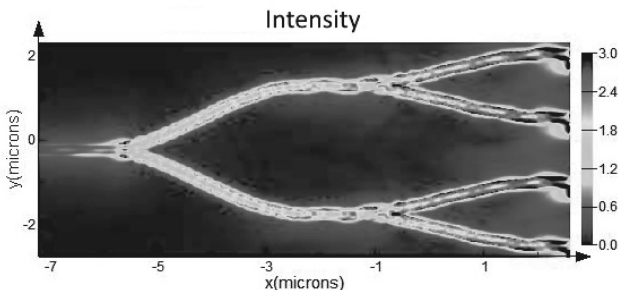


Fig. 4. The distribution of the SPP intensity within the four-channels multiplexer applied as an adder.

and 50 fs time interval between channels. The 50 fs time between pulses is chosen by experimentation. Thus time division of channels is applied. The distribution of SPP intensity in this scheme (as an adder) is shown in Figure 4.

The results suggest that the right distance was chosen between pulse duration and pulse signal which results in the correct form of the signal. The received signal strength is low due to ohmic losses and signal reflections in the middle of the waveguide, but enough to identify it.

## Experimental details

A glass substrate which will form the waveguide must be cleared first, because it affects the quality of the results. The glass surface was cleaned by ultrasonic waves directed from the generator in a bath filled with acetone. Glass immersed in acetone for 30 seconds. Then washed in distilled water.

To obtain a sample on a glass substrate, 50 nm thick gold deposition process was conducted in a vacuum. Silver deposited with thickness of 1  $\mu\text{m}$  was applied to manufacture a mask. Desired thickness of the metal film can be controlled by the time of deposition.

A template was created using application package CAD (CorelDRAW) to form channels of the corresponding configuration setting parameters of line thickness, a desired pattern in a circle of 20 cm radius is formed.

A pattern was printed with the ink-jet printer on a film. After the pattern was formed, a visual qualitative analysis of the unexpected or unnecessary sections of white lines had to be carried out.

The next step was the application of the positive photoresist S1813 mark by spin-coating. for quality application of photoresist and to obtain the desired height of polymer (1550 nm) it was necessary to follow certain parameters namely: the speed of rotation of the glass to set the spin-coating - 3000 rpm and rotating time of glass - 30 s. Graph of the height of the polymer forming dependance on the speed of rotation of glass is shown in figure 5.

After completing the process of application of the positive photoresist, the prototype had to be held at 115° for 50 s, then the process of polymerization could already begin, which was made using a light source with a wavelength of 410 nm and a lens in scale 1:10 (see Fig.6).

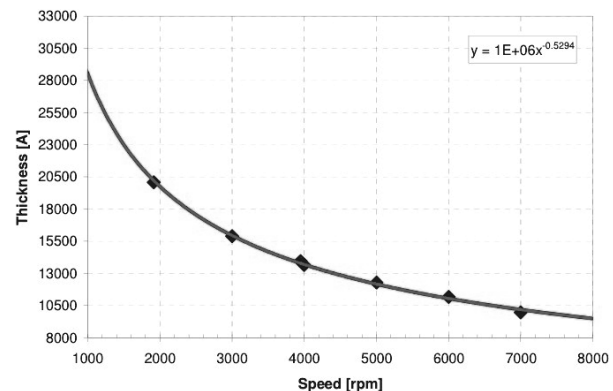


Fig. 5. The polymer thickness dependence (S1813) on the rotation speed of the glass [14]

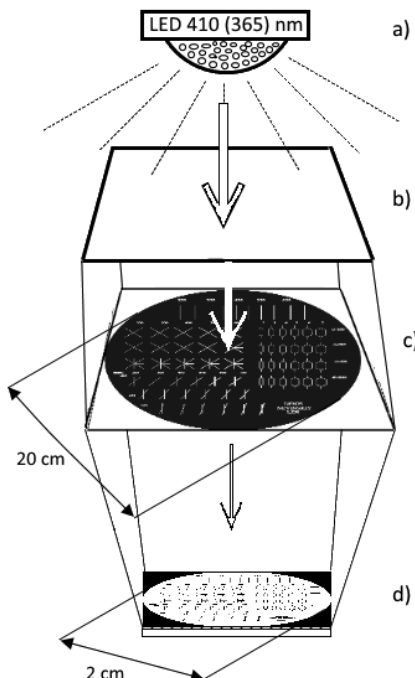


Fig. 6. Scheme of exposure process of waveguides images in the scale of 1:10 : a) light emitting diode with a wavelength of 410 nm; b) lens; c) pattern of 20 cm diameter; d) obtained mask 2 cm in diameter

To obtain a ready mask after irradiation with light, the polymerized polymer had to be removed with organic solvent (15 s), and after etching of silver - in hydrochloric acid (20-30 s).

The next step was the process to reduce the size of the waveguide to the scale of 1: 100 and to create a prototype. The process to make a prototype on gold is similar to the process of making a silver mask, but in this case the negative polymer was used (mark mr-NIL 6000.1E). light-emitting diode with a wavelength of 365 nm and a system of lenses were used as the source of illumination. polymer film with the thickness of 100 nm was deposited by The method of spin-coating. the rotation speed was 3000 rpm for 30 s [15]. After completing the polymerization process

polymerized polymer has to be removed in a solution of tree chloromethyl and experimental sample has to be rinsed in distilled water.

The resulting waveguides had the length of 50  $\mu\text{m}$  and a width of 150 nm to 450 nm (see Fig.7).

Figure 8 shows schematically the SPP excitation process. To excite an SPP, the laser with the wavelength of 632.5 nm and a pulse frequency of 250 fs was applied. Beam was directed perpendicularly to the top of the waveguide.

Figure 9a shows the SPP propagation in the formed linear waveguide using LR microscope [16]. The presence of this wave confirms the Fourier image on Figure 9b.

For the 150 nm wide waveguide the greatest intensity of SPP is observed at the distance of 10  $\mu\text{m}$  from the be-

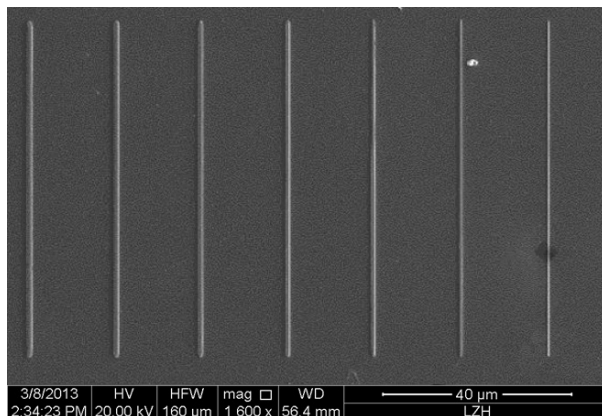


Fig. 7. Linear waveguides image of obtained waveguides made using an electron microscope.

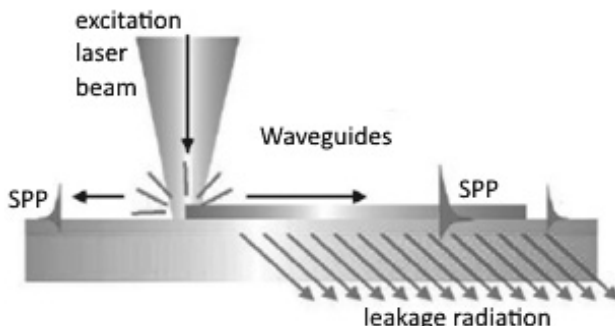


Fig. 8. Schematic representation of SPP excitation.

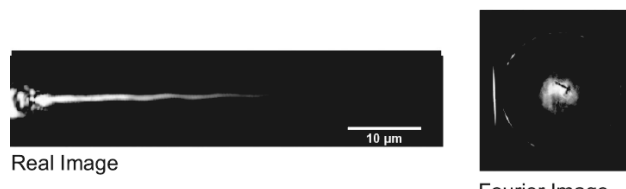


Fig. 9. Images made by LR microscope: a) SPP propagation through the waveguide, b) Fourier image

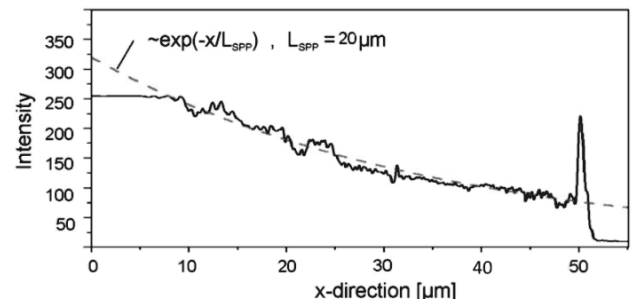


Fig. 10. The intensity of SPP propagation along the waveguide. The solid line — experimental data, dashed line — theoretical calculation of SPP attenuation

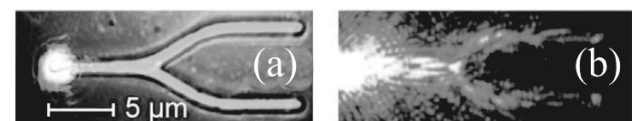


Fig. 11. The SPP propagation in dual channel splitter: a) – the image of the 20  $\mu\text{m}$  long splitter; b) – SPP propagation in the splitter made by LR microscope [16]

ginning of the excitation, respectively with the distance increase the SPP intensity decreases. The best case of SPP propagation was observed in the 200 nm wide waveguide while the highest intensity was on the path of  $\sim 20 \mu\text{m}$  (see Fig.10).

Figure 10 shows the SPP intensity: measured for the 200 nm thick waveguide (solid line) and calculated SPP attenuation (dashed curve) depending on the propagation length. The graph shows that the experimental results are consistent with theoretical calculations.

### Investigation of the SPP propagation in two-channel splitter

The above-described method employing optical lithography was chosen to create the two-channel multiplexer.

The 20  $\mu\text{m}$  long two-channel multiplexer was formed with the Width between the branches of 5  $\mu\text{m}$  and a thickness of 500 nm (see Fig.11a)

The SPP excitation was carried out with 632.8 nm laser and is held perpendicular to the entry of the splitter. The laser beam was focused in the center of the entry point of the splitter, as it shown in Figure 11a.

Figure 11b shows SPP propagation within the splitter. It is demonstrated that the SPP propagates in two-channels of the splitter on the entire length of 20  $\mu\text{m}$  and partially is attenuated by ohmic losses and split the SPP.

The investigated splitter properties open the possibility to create more splitters, including Four-channel that will be the light controlled. Application of these splitters is possible in nanocircuits where large signal losses occur when converting optical signals into electrical signals.

## Conclusions

The SPP propagation through the 10 μm x 5 μm four-channel multiplexer is simulated in the paper.

A phased optical lithography technology, which makes it possible to reduce the cost and simplify the process of obtaining the dielectric inhomogeneous structures to form nanoscale waveguide's is proposed in current paper. Samples obtained by optical lithography, have clear lines, steep walls od exposed or polymerized photoresist which confirms the ability to form a conductive channels of various configurations.

20 μm x 5 μm Two-channel multiplexer was formed by optical lithography to test the adequacy of the model. It is shown experimentally that the SPP divides into two-channels and passes with no significant attenuation to the end of the waveguide.

It was experimentally confirmed that the 150 nm wide waveguide's greatest intensity of SPP is observed at a distance of 10 μm from the beginning of the excitation and therefore SPP intensity decreases with a distance. The best case of the SPP propagation was observed in the 200 nm wide waveguide, high intensity distribution - 20 μm.

Figure 3 and 4 shows that the SPP fades during propagation in the multiplexer due to ohmic losses and the reflection in the mid-section of the multiplexer and split, but this intensity is sufficient to identify it on output.

The results presented in the Article will be employed to create compact elements for optical information processing, as well as a new class of devices for information and communication systems.

Thus the new four-channel multiplexer on SPP is obtained for processing and transmission of information in nanooptical schemes.

## Acknowledgments

Special thanks to the staff of the nanotechnology division, Laser Center Hannover (Laser Zentrum Hannover e.V.), Germany, for the opportunity to conduct experiments.

## References

- [1] Dellis S. et al.: Electrochemical synthesis of large diameter monocrystalline nickel nanowires in porous alumina membranes. *Journal of Applied Physics*, 114 (16), 2013 art. no. 164308.
- [2] I. P. Radko et al.: Spin-S Kitaev model: Classical ground states, order from disorder, and exact correlation functions. *Phys. Rev. B* 78, 115-116 (2008).
- [3] H. Liu et al.: Surface plasmon generation by sub wavelength isolated objects. *IEEE Journal of Selected Topics in Quantum Electronics*. 14, 1522–1529 (2008).
- [4] B. Wang et al.: Efficient generation of surface plasmon by single-nanoslit illumination under highly oblique incidence. *Applied Physics Letters* 94, 011-114 (2009).
- [5] A. B. Evlyukhin et al.: Asymmetric and symmetric local surface-plasmon polariton excitation on chains of nanoparticles. *Optics Letters* 34, 2237–2239 (2009).
- [6] S. I. Bozhevolnyi and J. Jung: Scaling for gap plasmon based waveguides. *Optics Express* 16, 2676–2684 (2008).
- [7] S. I. Bozhevolnyi et al.: Channel plasmon subwavelength waveguide components including interferometers and ring resonators. *Nature* 440, 508–511 (2006).
- [8] S. A. Maier, *Plasmonics—Fundamentals and Applications* (Springer, 2007).
- [9] A. V. Zayats et al.: Nano-optics of surface plasmon polaritons. *Phys. Rev.* 408, 131-314 (2005).
- [10] A. B. Evlyukhin, S. I. Bozhevolnyi.: Point-dipole approximation for surface polariton scattering: Implications and limitations. *Phys. Rev.* 71, 134-303 (2005).
- [11] A. B. Evlyukhin and S.I. Bozhevolnyi: Surface plasmon polariton scattering by small ellipsoid particles. *Surface science*. 590, 173-180 (2005).
- [12] C. Girard and A. Dereux: Near-field optics theories. *Rep. Prog. Phys.* 59, 657-699 (1996).
- [13] M. Paulus, P. Gay-Balmaz, and O.J.F. Martin: Accurate and efficient computation of the Green's tensor for stratified media. *Phys. Rev. E* 62, 5797 (2000).
- [14] D. Nevinskyi et al.: Two-Photon Polymerization: Formation of Nanoscale Elements. Conference on Modern Problems of Telecommunications, Computer Science and Engineers Training 2014, 283 – 285. (2014).
- [15] D.V. Nevinskyi et al.: Surface Plasmon-Polariton in X – Shaped Waveguides. Nanomaterials: Application & Properties-2014, (2014).
- [16] A. Drezet et al.: Leakage radiation microscopy of surface plasmon polaritons. *Materials Science and Engineering: B Volume* 149, Issue 3, 15 April 2008, Pages 220–229.

**Author(s): PhD student – assistant DENYS NEVINSKY – Lviv Polytechnic National University, Department of Electronics and Computer Technologies (ECT).**

**Associate Professor LUBOV ZAKALYK – Lviv Polytechnic National University, Department of Electronics and Computer Technologies (ECT).**

**Associate Professor SOLOMIA LEBID – Associate Professor of the European University.**

**Researcher KORZH HALYNA – Lviv Polytechnic National University, Department of Occupational Health (DOH).**

**Professor VOLODYMYR PAVLYSH – First Vice-rector Lviv Polytechnic National University, Department of Electronics and Computer Technologies (ECT).**

**Received:** 15 December 2015

**Received in revised form:** 12 February 2016

**Accepted:** 1 March 2016